Songklanakarin J. Sci. Technol.
33 (2), 237-246, Mar. - Apr. 2011

SJST SONGKLANAKARIN JOURNAL OF SCIENCE AND TECHNOLOGY
http://www.sjst.psu.ac.th

Original Article

Characterization of reservoir fractures using conventional geophysical logging

Paitoon Laongsakul and Helmut Dürrast*

Geophysics Group, Department of Physics, Faculty of Science, Prince of Songkla, University, Hat Yai, Songkhla, 90112 Thailand.

Received 6 November 2010; Accepted 30 April 2011

Abstract

In hydrocarbon exploration fractures play an important role as possible pathways for the hydrocarbon flow and by this enhancing the overall formation's permeability. Advanced logging methods for fracture analysis, like the borehole acoustic televiewer and Formation Microscanner (FMS) are available, but these are additional and expensive tools. However, open and with water or hydrocarbon filled fractures are also sensitive to electrical and other conventional logging methods. For this study conventional logging data (electric, seismic, etc) were available plus additional fracture information from FMS. Taking into account the borehole environment the results show that the micro-spherically focused log indicates fractures by showing low resistivity spikes opposite open fractures, and high resistivity spikes opposite sealed ones. Compressional and shear wave velocities are reduced when passing trough the fracture zone, which are assumed to be more or less perpendicular to borehole axis. The photoelectric absorption curve exhibit a very sharp peak in front of a fracture filled with barite loaded mud cake. The density log shows low density spikes that are not seen by the neutron log, usually where fractures, large vugs, or caverns exist. Borehole breakouts can cause a similar effect on the logging response than fractures, but fractures are often present when this occurs. The fracture index calculation by using threshold and input weight was calculated and there was in general a good agreement with the fracture data from FMS especially in fracture zones, which mainly contribute to the hydraulic system of the reservoir. Finally, the overall results from this study using one well are promising, however further research in the combination of different tools for fracture identification is recommended as well as the use of core for further validation.

Keywords: fractures, geophysics, well logging, reservoir characterization

1. Introduction

Fractures are of tectonic origin and can be described as more or less planar openings where one dimension (height) is smaller than the other two dimensions (length and width). They are mechanical breaks in rocks involving discontinuities in displacement across surfaces or narrow zones (Bates and Jackson, 1980). Fracture networks in a hydrocarbon reservoir are of importance as they can provide additional flow pathways for fluid and hydrocarbon transport (hydraulic fractures) or they can act as fluid flow barriers and therefore acting as seals, for example, when filled with clay or shale (see Figure 1). Hydraulic fractures are of great importance for hydrocarbon reservoirs, which have low to very low matrix permeability, so called tide reservoir rocks, as the open fractures provide additional secondary permeability. Therefore, fracture characterization is essential for assessing the success of exploration wells as well as for further production.

Due to the restricted accessibility of subsurface formations two main types of methods for fracture characterization are currently applied, surface and borehole geophysical methods. Shear wave splitting in seismic reflection is one main surface method for fracture characterization, which works under the principle that a shear wave propagating through a cracked rock splits into two, a fast shear wave polarized parallel to the strike of the predominant fracture

* Corresponding author.
Email address: helmut.j@psu.ac.th

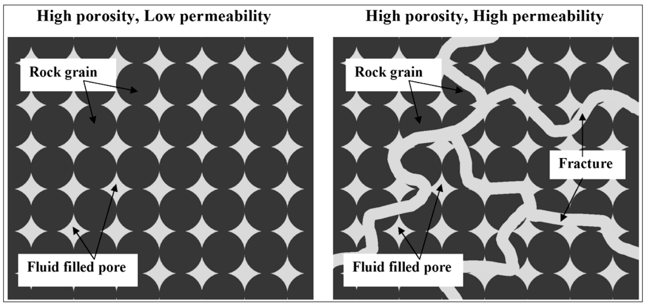

Figure 1. Fracture porosity increases permeability and fractures as fluids path way contribute to permeability. Left: without fracture; Right: with fractures.

orientation, and a slow one polarized perpendicular to it, which is time delayed by an amount proportional to the number of cracks per unit volume along the path between source and receiver (Crampin, 1981). In borehole methods, fractures are usually identified and evaluated by several techniques, mainly core analysis, conventional and advanced logging methods, like FMS (Formation Microscanner), BHTV (Borehole Televiewer), and DSI (Dipole Shear Imaging).

Coring of the subsurface formation is the preferred option to get required fracture information as cores are providing direct access to the subsurface. However, this option is expensive and relatively time consuming, which additionally adds to the costs. Therefore, usually geophysical logging methods are applied for subsurface fracture characterization. All methods have the advantage over coring that they are faster and by this saving time and money; but on the other side they do provide only indirect access to the subsurface formation through a physical measurement, which increases the uncertainties in fracture characterization.

Conventional logging methods for fracture characterization comprise of gamma ray tool (NGR), sonic tools, shallow and deeper reading resistivity tools, photoelectric log, caliper log, and temperature log. They are briefly described below; more details for all methods can be found by Ellis (1987), Serra (1988), Ellis and Singer (2008), and Crain (2010).

1) The gamma ray tool is measuring the natural gamma ray emission from the decay of Potassium, ^{40}K, Thorium, ^{232}Th, and Uranium, ^{238}U, usually found in clay minerals. Most of the Uranium compounds are soluble in both water and hydrocarbon and by this they can penetrate into fractures zones where an enhanced permeability is. The subsequent precipitation of U–containing minerals results in a higher gamma ray reading of the fractures.

2) The sonic tool is measuring the travel times or transit times of the compressional and the fastest shear waves of the formation parallel to the borehole wall by utilizing the seismic refraction technique. From this the P– and S–wave velocities, Vp and Vs, respectively, are determined, usually presented in slowness (ms/m) as the reciprocal of the seismic velocity. In general, compressional waves are less affected by single factures or fractured parts of a formation than shear waves. Fractures strongly attenuate the shear wave energy resulting in smaller amplitudes and in an increase in the travel time of the shear waves. Fluid filled fractures even contribute to a stronger attenuation.

3) In the presence of open fractures the mud filtrate penetrates from the borehole into the fracture space and by this deeper into the formation. If then the resistivity contrast between the mud filtrate resistivity and the formation resistivity is great enough then electrical logging tools reading deeper will indicate the fracture zone. Shallow reading electrical tools (e.g. microlog, ML, and micro spherical focused log, MSFL) might indicate open fractures zone with lower resistivity readings in case of a highly conductive mud filtrate. Higher resistivity values are expected opposite healed or mineralized fractures.

4) The photoelectric log or density tool is measuring the photoelectric absorption of gamma rays by electrons. Barite, as a compound in mud used for density increase, has a very large photoelectric cross section and therefore a high photoelectric absorption index (Pe). Barite loaded mud penetrates into open fractures and resulting in sharp peaks of the Pe–curve in front of a fracture filled with barite containing mud.

5) The caliper tool measures the size of the borehole diameter usually applying four or six arms. Any increase in the borehole diameter from the diameter drilled might indicate larger fractures or fracture zone. However, mechanical soft rocks or soluble formation can also exhibit increases in the borehole diameter, e.g. washout.

6) The temperature log is providing a continuous temperature profile of a borehole, with the temperature in general increasing with depth. Open fractures might exhibit fluid inflow into the borehole, which results in a decrease in the temperature of this borehole section.

Advanced logging methods for fracture characterization available today are the Formation Microscanner or Formation Micro–Imager (FMI), Borehole Televiewer, and Dipole Shear Imaging.

7) The FMS or FMI tool comprises several pads, which will be attached to the borehole wall during operation. Each pad contains several micro–resistivity tools providing altogether a resistivity “image” of the shallow borehole wall, showing different resistivity values in different gray shades or colors (Figure 2). Fluid filled fractures will show lower resistivity; whereas hydrocarbon filled fractures will exhibit higher resistivity values.

8) The borehole televiewer tool employs a rotating acoustic transducer emitting highly focused ultrasonic waves radial outwards in the direction to the borehole wall. The same transducer then measures the wave reflected from the borehole wall, its amplitude and travel time. This information, combined with orientation data provides an extremely detailed acoustic image of the borehole wall. Open fracture do not reflect the acoustic waves back and appear usually black in the colored images (Figure 3).

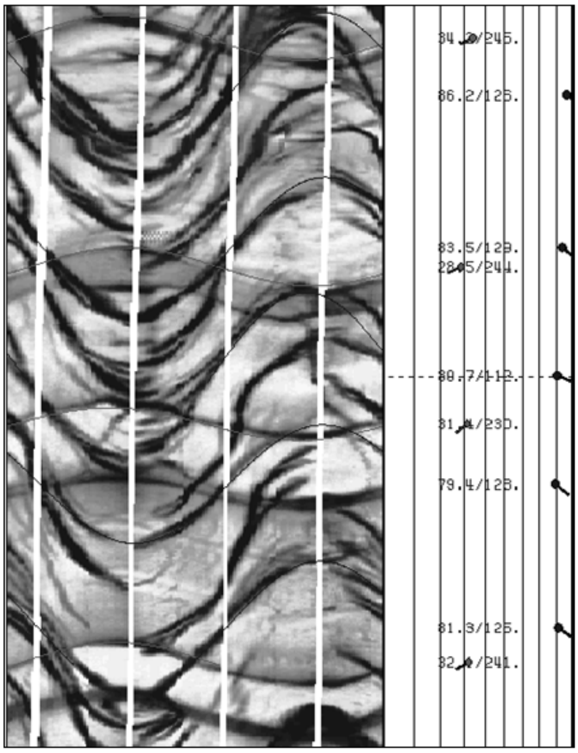

Figure 2. Example of an FMI image with dipping fractures relative to the borehole axis as sinus curves. On the right showing the processed data with dip direction and dip angle (after HEF, 2011). Note that the image is not from this study.

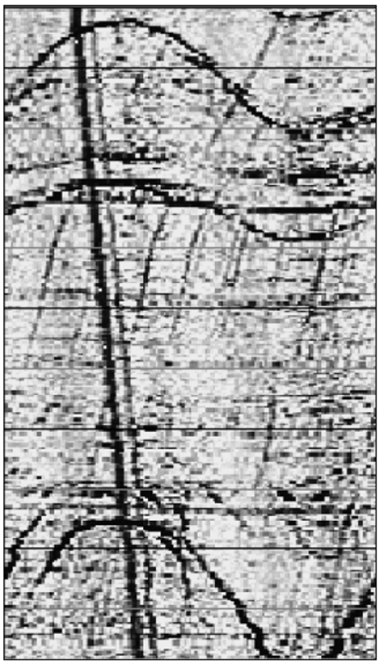

Figure 3. Example of an BHTV image with dipping fractures relative to the borehole axis as sinus curves (after Deltombe and Schepers, 2001). Note that the image is not from this study.

Both, the BHTV and FMI tool provide "images" of more or less the whole borehole wall and by this reveal more fracture characteristics. Factures dipping relative to the borehole axis, as well as other structural geological features, appear in these images as full sinus curves, with the minimum (wave trough) indicating the dip direction in degrees from north as the tools are usually oriented in the magnetic reference system. From the amplitude of the sinus waves the dip angle can be calculated. Hydrocarbon filled or mineralized fractures appear in the FMS image as sinus curves with higher resistivity fractures whereas water filled fracture appear as sinus curves with higher conductivity.

9) The DSI (Dipole Shear Imaging) tool comprises monopole and crossed–dipole acoustic transmitters, which excite compressional- and shear-waves in the formation, and multi receivers. The crossed dipoles allow the investigation of shear wave spitting effects as a result of preferred oriented (vertical) fractures in the formation.

Advanced logging tools are the preferred choice for fracture characterization as they provide less ambiguous information and more data for further fracture characterization, e.g. dip direction, dip angle, or resistive (hydrocarbon filled or mineralized fracture) and conductive (water filled fracture) for the FMI. However, these tools are additional tools so that their applications require more time, which adds to the generally higher operational costs. Applying conventional logging for fracture characterization is desirable where reservoirs are separated into smaller structural hydrocarbon traps, like in the Gulf of Thailand. Each small structure requires a well to be drilled, but with a comparable small production. In this situation not much money will be spend for advanced logging. More information about the subsurface formation, here about fractures, from the standard logging tools might be useful and less expensive, as standard tools are usually applied to every well to get necessary petrophysical and engineering information. This study will evaluate the potential of conventional logging methods to identify fractures in a well drilled in a fractured clastic reservoir.

2. Material and Methods

2.1 Logging data

For this study logging data were provided by a petroleum company from one well of a clastic reservoir with three main lithologies, sandstone, shale, and coal. The well was drilled with conductive mud. The mud temperature near surface is 18°C with about 0.075 Ωm for the mud resistivity and at 100°C, representing increasing depth, the mud resistivity is about 0.025–0.038 Ωm. Three data sets, all from the same one well, are used in this research. The borehole orientation is not available.

The first data set (Log 1) is measured between 2679.954-3694.938 m, with a sampling interval of 15.2 cm. It comprises measured and already processed (calculated) data, with MSFL (electrical resistivity measured by micro spherical focused log), LLd (electrical resistivity measured by a deeper reading laterolog), LLs (electrical resistivity measured by a shallow reading laterolog), CALI (caliper log measured the hole size), GR (natural gamma ray measurement), DTc (compressional wave slowness data), PEF (photoelectric absorption data), RHOB (calculated bulk density), SS (calculated sandstone content), SH (calculated shale content), COAL (calculated coal content), and NPOR (calculated neutron porosity). Processing and calculations were done by the company, ready to be used for this study. Details about the data processing and calculations of logging data in general can be found by Serra (1988), Ellis and Singer (2008), and Crain (2010).

The second logging data set (Log 2) is measured between the depths 2699.995 m and 2931.998 m, with a sampling interval of 2.5 cm, including of GR, DTc (see above), and DTs (shear wave slowness measurement). The last data set (Log 3) is based on interpreted FMS logging data; however the original FMS data were not used here. Log 3 comprises of following processed data from the FMS tool, depth of fracture and type, either conductive or resistive fracture, as it is basically a resistivity tool. The FMS images and further processed data from the tool were not available for this study.

Note the depth data presented here are not the real depth data of the well, but for all three data sets the depth values are comparable. This has no effect on the results and conclusions drawn from the data.

2.2 Measurement techniques of logging tools

The GR log is a measurement of the natural radioactivity of the formations. It is mainly used for determining the location of shale and non-shale beds, and for general well correlation. Natural gamma ray logs tend to have a shallow depth of investigation, less than 30 cm, and will give a depressed respond opposite large open fractures with a low gamma count (Ellis, 1987). Density logs are primarily used as porosity logs. The investigation depth of a density log is shallow, so mud cake and borehole rugosity can have an appreciable effect on the total measurement, despite the fact that it is a pad type contact device with some borehole compensation applied. However, if the density log shows low spikes reading, usually fractures, large vugs, or caverns exist (Czubek, 1983).

Sonic logs measure the travel time of the elastic waves from the transmitter to the formation and refracted back to the receiver. In the case of well logging, the borehole wall, formation bedding, borehole rugosity, and fractures can all represent significant acoustic discontinuities. In some situation, fractures can attenuate the sonic signal to the extent that only second or third arrivals are detected by the receiver, thus wave cycles are missed or skipped, and the logs show up as abrupt increases in the interval transit time (Keys, 1988).

Resistivity logs include MSFL, LLd, and LLs, which measure the resistivity of the formation in different depth of investigation. The MSFL may read the resistivity close to drilling mud in washed out borehole sections caused by the presence of fracturing (Schlumberger, 1989). The LLs is reading shallow in the formation, whereas LLd is reading deeper. The caliper log measures the average holes size by using caliper arm, which are connected to variable resistance push along to borehole wall and the changing electric signal can be translated into holes size (Serra, 1979; Rider, 1986). The photoelectric (PE) absorption property depends on the composition of lithology. Normally it is used for coal content determination, but when barite containing mud is used a larger PE value greater than 5.0 can be used as a fracture indicator (Crain, 2010). Barite has a very large photoelectric cross section (267) and therefore the PE curve should exhibit a very sharp peak in front of a fracture filled with mud. The neutron porosity (NPOR) is derived from a neutron log that emits neutrons from a source usually at the bottom of the tool and then measures decrease rate of the neutron density with distance from a source, where the rate mainly depends on the hydrogen content of the formation. With a calibrated tool this rate can be converted into an apparent porosity value (Serra, 1988).

2.3 Borehole environment

During the drilling of the well the hydrostatic pressure of the mud column is usually greater than the pore pressure of the formations for prevents the well from blowing out. The resultant pressure difference between the mud column and formation forces mud filtrate into the permeable formation and the solid particles of the mud are deposited on the borehole wall and form a mud cake (Figure 4). Very close to the borehole most of the original fluid formation may be flushed away by the filtrate. This zone is referred to as the flushed zone. Further out from the borehole into the formation, the displacement of the formation fluids by the mud filtrate is less and less complete, resulting in a transition from mud filtrate saturation to original formation water saturation. This zone is referred to as the transition or invaded zone. The undisturbed formation beyond the transition zone is referred to as the uninvaded zone (see Figure 4).

2.4 Fracture parameters

The main fracture parameters are fracture size, orientation, type of fracture (open, closed, mineralized), and in case of an open fracture the fluid type in the fracture (water, hydrocarbon), as shown in Figure 5. The resolution of the logging data sets the limit of the fracture detection. Log 1 has a sampling interval of 15.2 cm, whereas Log 2 has an interval of 2.5 cm; with the depth interval of Log 2 much smaller than for the first data set (see Section 2.1). However, significant hydraulic fractures often come as sets of parallel fractures rather than in single fractures (Aguilera, 1995), so

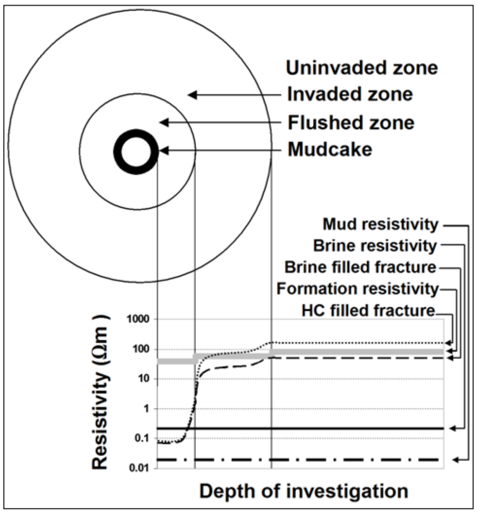

Figure 4. Schematic diagram of the borehole environment including mud cake, flushed zone, invaded zone, and uninvaded zone, and a qualitative transition profile of the electrical resistivity (ohm m) when a fracture is present (hydrocarbon or brine filled) of a sandstone formation with porosity <5%.

that a sampling interval of 15.2 cm (Log 1) might be sufficient for detecting the fractures; however not all fractures will be detected using this sampling interval. With shorter intervals the possibilities of detecting more fractures increase. Fractures that are oriented parallel to the borehole axis cannot be detected by the logging tools unless they cut directly through the borehole wall. Therefore, fractures with an angle to the borehole axis are detectable. However, usually the borehole axis is not vertical, so vertical fractures also can be detected when the borehole itself is inclined. Fractures can be either open or mineralized, with the later one acting as a barrier or seal and by this preventing fluid flow. Usually more important are the open and hydraulic fractures that enhance the fluid flow, and then to separate hydrocarbon (oil or gas) from water (brine) filled fractures.

2.5 Geophysical signature of main lithologies

In order to see any changes in the logging data related to the presence of fractures the geophysical signature of the three main lithologies has been determined. Usually, sandstone and shale and shale and coal are mixed or interbedded with various percentages of one or the other lithology. Therefore a lithology content value of higher than 75% was assigned for the main formations to describe a main lithology, as a higher value would limit the available data. For example, if lithology composed of sandstone 75%, shale 20%, and coal 5%, this layer is assigned to be sandstone formation, although it also contains coal and shale. The average value and standard deviation from the conventional logging data values was determined for shale and coal (see Table 1). Further, the sandstone formation was separated in to three different porosity classes, (a) smaller than 5%, (b) between 5% and 10%, and (c) higher than 10% (see Table 1), as the porosity has a significant effect on various petrophysical properties, like resistivity or seismic velocities (see Schön,

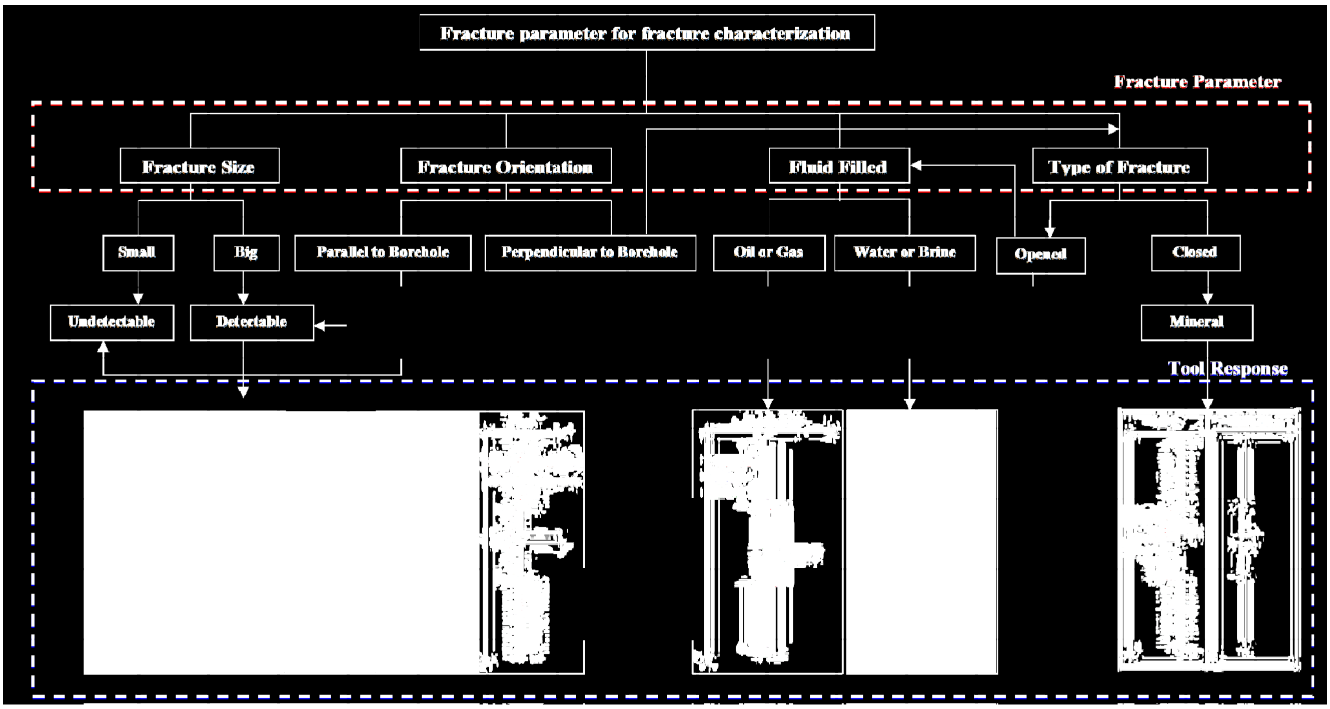

Figure 5. Flow chart for the qualitative fracture response for the different fracture parameters and for the available conventional logging tools. Further explanation in the text.

Table 1. Average and standard deviation values of various logging tool data for shale, coal, and sandstone formation with a lithology content ≥75%, and for the sandstone formation separated by different porosity values.

	GR (API)	RHOB (g/cm^3)	DT (us/ft)	MSFL (Ωm)	LLd (Ωm)	LLs (Ωm)	CALI (inch)	PEF (barns/e)	NPOR (vol/vol)
SHALE									
Average	149	2.67	65.8	50	111	91	7.1	3.7	0.14
STDEV	30	0.17	8.0	30	80	80	1.0	0.6	0.05
COAL									
Average	48	1.58	111.2	2	79	39	8.8	1.7	0.39
STDEV	40	0.23	10.0	5	160	40	0.9	1.1	0.10
SANDSTONE (all)									
Average	50	2.57	63.7	28	72	54	8.4	2.6	0.03
STDEV	10	0.07	4.0	20	40	40	1.0	0.3	0.01
Sandstone – porosity < 5%									
Average	57	2.62	60.4	39.3	84.9	66.6	7.8	2.7	0.03
STDEV	10	0.05	4.0	20.0	60.0	50.0	1.3	0.3	0.02
Sandstone – 5% ≤ porosity ≤ 10%									
Average	45	2.53	65.9	21.4	65.3	46.6	8.8	2.6	0.03
STDEV	10	0.04	2.0	10.0	30.0	20.0	1.0	0.3	0.01
Sandstone – porosity >10%									
Average	42	2.51	70.4	13.2	39.7	23.7	9.6	2.5	0.04
STDEV	5	0.11	4.0	10.0	20.0	10.0	1.8	0.5	0.01

1996). The average value of the main lithology represents the response of conventional logging data to an unfractured zone or the geophysical signature of the formations without fractures.

2.6 Qualitative logging response to fracture

To identify fractures with conventional logging data following approach is used in this study: using the qualitative response of the logging tools to the existence of fractures in general as described above, combining all the available tools available for this study, then taking into account the borehole environment, in order to indentify the location (depth) of fractures and if possible to characterize them further (mineralized, fluid filled).

The borehole environment is important for the logging response of porous formations such as sandstone. In order to understand the response of resistivity logs a transition profile of the formation and fracture in the sandstone formation has been established (see Figure 4: sandstone formation, porosity less than 5%). Sandstones with different porosity values are separated as their petrophysical signature is different. The transition model combines the borehole, the flushes zone, invaded zone and the virgin formation beyond the invaded zone. The mud resistivity of the well is used and a general brine resistivity of 0.3 Ωm. The transition model includes the formation resistivity with some uncertainty depending on the data in Table 1 (average with standard deviation), and the resistivity profile of brine and hydrocarbon filled fractures (Figure 4). The presence of a fracture reduces the resistivity in the flushed zone almost down to the mud resistivity value. A brine filled fracture reduces the resistivity in the invaded zone, whereas for a hydrocarbon filled fracture the resistivity in this zone should be close to the formation resistivity. In the flushed zone the resistivity of the hydrocarbon (HC) or brine filled facture is comparable due to the invasion of the low resistivity mud filtrate.

The qualitative response for open fractures can be summarized as following as shown in Figure 4 and 5:

- Caliper – fracture increases borehole diameter,
- RHOB – density is lower due to the existence of a fracture, (brine filled fractures slightly above 1 g/cm^3),
- DTc – slightly increase in the slowness (decrease in velocity) or no effect,
- DTs – (significant) increase in the slowness, more than DTc,
- DTs/DTc – increase in the slowness ration due to

the increase in DTs, however the ratio takes also into account any increase in DTc slowness due to other formation parameters (lithology, porosity, etc.),

- PEF – assuming a barite loaded mud the PEF value increases due to the presence of a fracture,
- MSFL – more or less similar for HC and brine filled fractures due to the invasion of low resistivity mud into the fracture; the invasion depends also on the mud weight,
- LLs – for HC filled fractures slightly higher resistivity values and for brine filled slightly lower values related to the flushed and invaded zone,
- LLd – for HC filled fractures slightly higher resistivity values than LLs readings and for brine filled slightly lower values than LLs related to the deeper invaded zone.

The qualitative response for mineralized fractures can be summarized as following as shown in Figure 5:

- RHOB – density is equal or slightly higher due to the existence of a mineralized fracture filling,
- DTc – slightly decrease in the slowness (increase in velocity) or no effect,
- DTs –(significant) decrease in the slowness, more than DTc,
- DTs/DTc – decrease in the slowness ration due to the decrease in DTs, however the ratio takes also into account any decrease in DTc slowness due to other formation parameters (lithology, porosity, etc.),
- Other parameters do not apply to mineralized fractures.

The available FMS data in this study, depth of fracture and resistive or conductive type, were used as a reference for fracture locations in the well, in order to see how good the conventional tools can identify the fracture locations. However, as explained above, the FMS can see more fractures due to a measurement interval of 0.25 cm (Serra, 1988). The conventional logging data were combined with the FMS fracture data applying the qualitative response of the different logging tools, which serves as an explanatory example. All available logging data were used in the analysis, but only representative examples are show here.

3. Results and Discussions

3.1 Fracture identification

Figure 6 shows a single conductive fracture (CF) present at a depth of 2716.378 m in a formation with 72.5% sandstone, 27.1% shale content and 0.4% porosity. The log data show that the very shallow resistivity log MSFL reads a value of about 13 Ωm, lower than the general formation; however the interval of the lower MSFL value is about 30 cm. The ΔTs/ΔTc ratio is higher than the formation with 1.73 due to the slight increase in DTs, which by itself seems not significant. But the ΔTs/ΔTc ratio shows a significant increase with a clear spike at the fracture location derived from the FMS log. The photoelectric absorption at the fracture location is with 3.2 barns/ê higher than at the formation above and below, but with a broader depth interval of about one meter. Also the NPOR shows a higher value with a broader peak around the fracture. Both support a fractured zone with water filling above and below the fracture indicated by the FMS.

Figure 7 presents at 3409.645 m depth a conductive fracture inside a formation of sandstone (55.4%) and shale (44.6%) and with no porosity (0%). The MSFL reading is with 5 Ωm significantly lower than above and below the fracture with a clear spike. The LLs with 24 Ωm and LLd with 31 Ωm are slightly lower indicating a water filed fracture rather a hydrocarbon filled one. The DTc shows a relatively clear increase around the fracture location (200.3 µs/m), which means that the rock mass here must be considerably fractured in order to reduce significantly the P–wave velocity. This coincides with a significant decrease in the RHOB values, down to 2.66 g/cm^3 from around 2.70 g/cm^3. The photoelectric absorption does not show a significant change at the fracture location.

Figure 8 shows a single resistive fracture present at a depth of 2830.068 m in a formation with 82.3% sandstone, 14.7% of shale and a porosity of 3.0%. The MSFL reading gives a very low resistivity with 3 Ωm with a broader peak

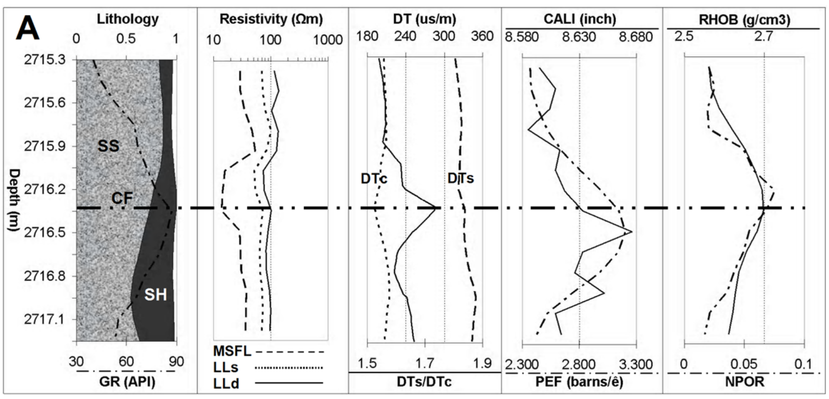

Figure 6. Fracture analyses in the depth interval between 2715.3 m and 2717.1 m.

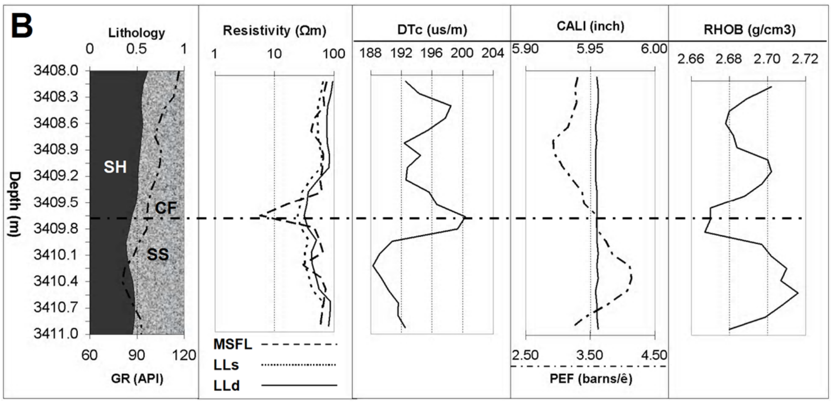

Figure 7. Fracture analyses in the depth interval between 3408.0 m and 3411.0 m.

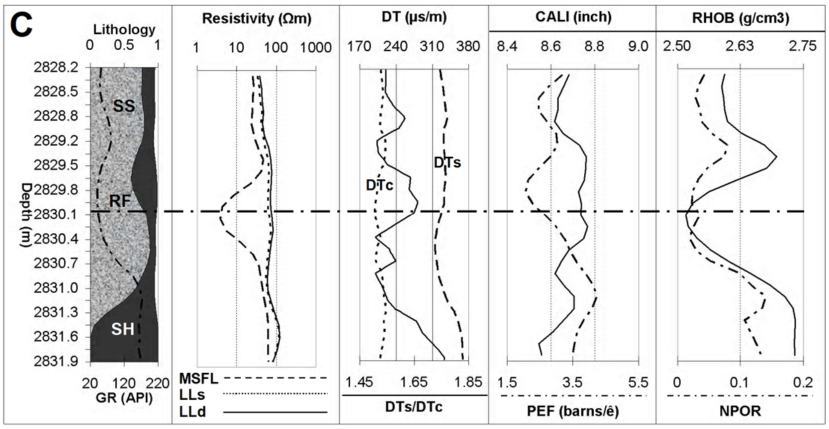

Figure 8. Fracture analyses in the depth interval between 2828.2 m and 2831.9 m.

than 3409.645 m depth. LLs is about 66 Ωm and LLd is about 76 Ωm. Both readings slightly increase indicating a resistive hydrocarbon filled fracture rather than a water filled one. The compressional and shear wave slowness are 202.0 µs/m and 334.0 µs/m, respectively. Although both values, DTs and DTs, show almost no changes the ΔTs/ΔTc ratio exhibits a broader increase with a peak increase (1.68) at the fracture location. The photoelectric absorption value PEF shows a lower trend around the fracture location with the peak slightly above supporting a hydrocarbon filled fracture. NPOR and RHOB both show a significant decrease around the fracture location, with the bulk density having a lowest value of 2.51 g/cm^3.

3.2 Fracture index

The various log derived fracture indicators discussed and shown above can be merged, which allows a wider variety of inputs from all available logging data. The input curves are assigned a threshold value, a median value, and a maximum probability value to detect a fracture. In addition, each input is weighted according to its potential to identify fractures in a formation (see Crain, 2011). In this study, the weighting is assigned to the MSFL, DTc, RHOB, CALI, and PEF tool as all these tools are suitable fracture indicators (see above). The output is a fracture probability curve or fracture index. Figure 9 and 10 show the results of fracture index by using the following equation:

$$\text{Fracture index} = A\times((\text{DTc}>\text{Average}+\text{Stdev}) + B\times(\text{MSFL}<\text{Average}-\text{Stdev}) + C\times(\text{RHOB}<\text{Average}-\text{Stdev}) + D\times(\text{CALI}>\text{Average}+\text{Stdev}) + E\times(\text{PEF}>\text{Average}+\text{Stdev})) / N$$

where *Average* is the average log value for a formation (see Table 1), *Stdev* is the related standard deviation (see Table 1), *A to E* are the weighting, here all equal 1, which means all logs have the same weight, and *N* is the number of thresholds tested or tools used, here N=5. The result is normalized between 0.0 and 1.0 by the number of thresholds tested. For example, a DTc log value above average value plus one standard deviation will indicate a fracture. For MSFL, RHOB the values must be below average value minus one standard deviation.

Figure 9 shows the result of the thresholds test for a sandstone layer between 2790 m and 2830 m depth. The

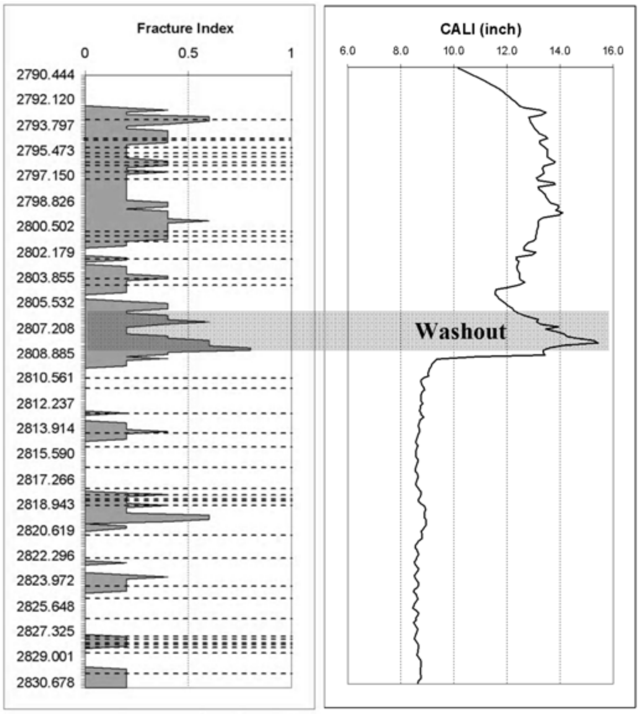

Figure 9. Correlation of the fracture index with fractures data from FMS in the depth interval between 2790.444 m and 2830.678 m.

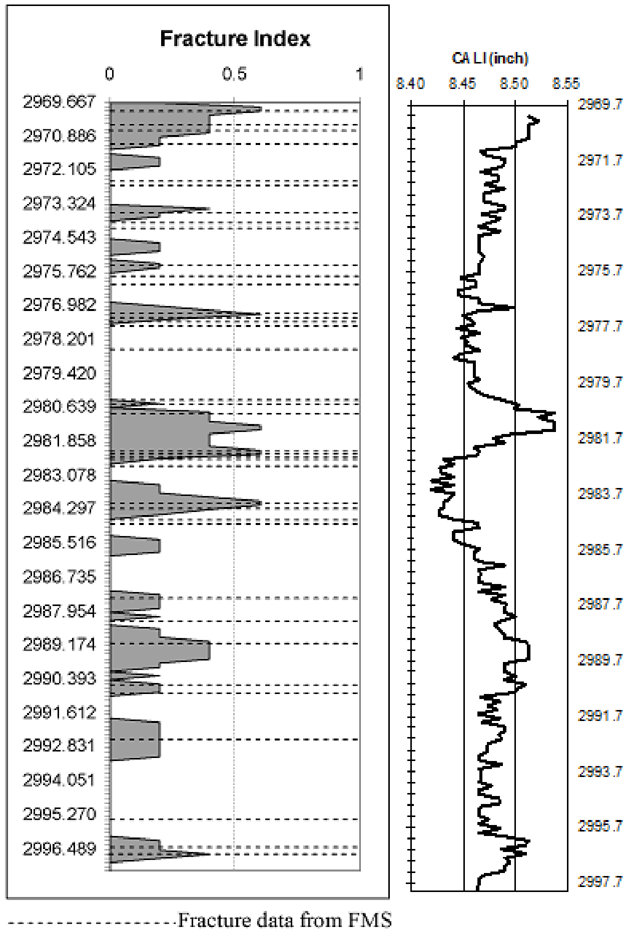

Figure 10. Correlation of the fracture index with fractures data from FMS in the depth interval between 3589.2 m and 3591.3 m.

fractures index correlates quite remarkable with the fracture data from the FMS when considering fracture zones, having several fractures in a shorter depth interval. Single fractures are more often missed by the threshold test.

At the depth interval between 2805.5 m and 2809.0 m the fractures index indicates significant fractures but no fractures are present in the FMS data. The reason for this comes from the borehole enlargement, so called washout or breakout, as indicated by the caliper log. As the caliper log is part of the threshold test these washouts will be regarded as fractures. Therefore, the fracture index has to be rechecked with the caliper log afterwards, as the caliper log is an essential part in the threshold test.

Figure 10 shows the fracture index correlated with fracture data from the FMS in the depth intervals between 2969.667 m and 2997.251 m, also a sandstone layer. The quality of the correlation between the threshold test data and FMS fracture location is similar as described above. Between 2980.7 m and 2982.4 m the fracture index shows fractures, but the FMS not. Here also a washout indicated by higher caliper values can be seen as the cause for this. Further, around 2989 m depth the fracture index might also correlate to the washout rather than fractures.

4. Conclusions

From the result and the discussion above it can be concluded that conventional logging data can be successful applied for fracture identification and characterization, however with limitations. Using conventional logging data it is possible to identify the location of a fracture and to separate between conductive and resistive fracture. The main logging response in detail: At an open fracture the RHOB is reading lower than normal in front of the fracture, while DTc, DTs, and the ratio of $\Delta Ts/\Delta Tc$ is increasing. MSFL shows a low reading value close to mud the resistivity, whereas LLs and LLd may be affected by showing a very small anomaly, which can be used to identify fluid filling, resistive hydrocarbon or conductive brine/water. The PEF increases due to the penetration of mud loaded barite into the open fracture. The fracture index calculation using threshold and input weight also can be successful used to characterize open fractures especially fracture zones. However, any washout has to be ruled out using the caliper tool. Finally, this study has confirmed that conventional logging has a good potential to be used in fractured reservoir characterization, although no success rate can be given here due to the comparison with the FMS, which has a higher resolution than conventional logging tools. For further work it would be preferable to have core data for a correlation as cores would provide a realistic picture of the fracture parameter.

Acknowledgments

Most of the geophysical logging tools mentioned are registered trademarks of several companies, which is acknowledged herewith for the whole article. The authors would like to thank the Department of Physics and the Graduate School, Prince of Songkla University, for financial support, and an oil and gas exploration company for providing conventional logging data. The paper was presented at the 5th International Conference on Applied Geophysics in Phuket, Thailand, 11-13 November 2010.

References

Aguilera, R. 1995. Naturally Fractured Reservoirs, PennWell Books, Tulsa, Oklahoma, U.S.A.

Bates, R.L. and Jackson, J.A. 1980. Glossary of geology. 2nd edition, Falls Church, Va., American Geological Institute, pp 749.

Crain, E.R. 2010. Crain's Petrophysical Handbook. Mindware Ltd., Canada.

Crampin, S. 1981. A review of wave motion in anisotropic and cracked elastic media. Wave Motion, 343-391.

Czubek, J.A. 1983. Advances in gamma–gamma logging. In: C.G. Clayton, Editor, Nuclear Geophysics, Selected Papers on Applications of Nuclear Techniques in Mineral Explorations, Mining and Process Control, Pergamon Press, Exeter, 153–172.

Deltombe, J.-L. and Schepers, R. 2001. Combined Processing of BHTV Traveltime and Amplitude Images. The Minerals and Geotechnical Logging Society (MGLS) News. October, 1–13.

Ellis, D.V. 1987. Well Logging for Earth Scientists. Elsevier, New York, pp. 532.

Ellis, D.V. and Singer, J.M., 2008. Well logging for Earth Scientists. 2nd Edition. Springer, Berlin, Germany.

HEF, 2011. Borehole Image Generation and Interpretation, FMI Image. HEF Petrophysical Consulting, Inc., Calgary, Canada. http://www.hef.com/websiite/borehole5.htm [June 25, 2011].

Keys, W.S., 1988. Borehole geophysics applied to ground water investigations. United States Geological Survey. U.S.A.

Rider, M.H. 1986. The geological interpretation of well logs. John Wiley & Sons, Inc., New York, pp. 175.

Schlumberger. 1989. Log Interpretation Principles/Applications. Schlumberger Educational Services. Houston, Texas, pp. 250.

Schön, J.H. 1996. Physical properties of rocks: Fundamentals and principles of petrophysics. Vol. 18, Handbook of Geophysical Exploration, Seismic Exploration, Series editors, K. Helbig and S. Treitel, Pergamon Press, Elsevier, U.K.

Serra, O. 1979. Fundamentals of well–log interpretation. The acquisition of logging data: Elsevier Science Publishers, Amsterdam, The Netherlands.

Serra, O. 1988. Fundamental of well-log interpretation. Developments in Petroleum Science, Elsevier Science Publishers, Amsterdam, The Netherlands.